LOCAL VERSUS GLOBAL DUCTILITY DEMANDS IN SIMPLE BRIDGES

By Farid Alfawakhiri,[1] and Michel Bruneau,[2] Member, ASCE

ABSTRACT: This paper addresses the inelastic dynamic response of simply supported bridges to ground motion in their transverse direction. The effect of the relative substructure-superstructure flexibility on the inelastic response of bridges was studied for symmetric spans. The bridges are modeled as beams with distributed mass and elasticity, simply supported at the ends by elasto-plastic springs. An analytical extension of the common generalized single degree of freedom model into the inelastic range is presented. Flexibility of the capacity-protected structural elements is shown to add significantly to the ductility demand of the energy dissipating components of bridge systems. A simple method was developed to account for these flexibilities when assessing bridge response beyond its elastic range. Numerical case studies are presented to illustrate the new analytical tool.

INTRODUCTION

Complex nonlinear inelastic models have been used for seismic analysis in major bridge projects (e.g., Dameron et al. 1995; Ballard et al. 1996; Donikian et al. 1996; Ingham et al. 1996; Vincent et al. 1997). For most bridges, however, the simplified analytical procedures provided in current seismic provisions (*Standard* 1996) are generally followed. Furthermore, for simplicity, in the structural analysis of bridges for earthquake forces, engineers frequently assume infinitely rigid superstructures, particularly when using the uniform load method or when evaluating ductility demands in bridge supports. There is little guidance provided describing how unaccounted flexibilities can affect the dynamic response of bridges and when such effects become significant. In some instances superstructure flexibility can significantly increase the ductility demand imposed on bridge piers. Likewise, substructure flexibility can increase ductility demands in special end-diaphragms designed to exhibit ductile behavior and dissipate seismic energy.

With the exception of inelastic time-history analysis, all ''simplified'' analytical methods in current bridge design specifications (*Guide* 1991; *Bridge* 1993; *Standard* 1996), being formulated without distinction between member ductility demands and system ductility demands, implicitly permit nonconservative designs by neglecting the impact of flexible nonyielding elements on the ductility demands of the energy dissipating components. Priestley et al. (1996) points out this inconsistency and suggests corrective actions to account for the flexibility of substructure components. These measures still neglect the effect of superstructure flexibility on local ductility demands in bridge systems.

For this paper, a simple method predicts the local ductility demands of energy dissipating structural elements while properly accounting for the relative flexibility of the capacity-protected sub- or superstructure. Focus is on the inelastic dynamic response of symmetric simply supported bridges subjected to transverse ground motion. Numerical examples are provided to illustrate the analytical procedure for a ductile diaphragm application and for a more conventional bridge pier-yielding strategy, and to assess the accuracy of the method.

[1]Res. Fellow, Canadian Steel Construction Council, Inst. for Res. in Constr., Nat. Res. Council of Canada, Montreal Road, Ottawa, Ontario K1A 0R6, Canada. E-mail: farid.alfawakhiri@nrc.ca

[2]Prof. and Deputy Dir., Multidisciplinary Ctr. for Earthquake Engrg. Res., 105 Red Jacket Quadrangle, State University of New York at Buffalo, Buffalo, NY 14261-0025. E-mail: bruneau@ascu.buffalo.edu

Note. Associate Editor: Takera Igusa. Discussion open until October 1, 2001. To extend the closing date one month, a written request must be filed with the ASCE Manager of Journals. The manuscript for this paper was submitted for review and possible publication on December 8, 1999; revised January 2, 2001. This paper is part of the ***Journal of Structural Engineering***, Vol. 127, No. 5, May, 2001. ©ASCE, ISSN 0733-9445/01/0005-0554–0560/$8.00 + $.50 per page. Paper No. 22172.

LOCAL VERSUS GLOBAL DUCTILITY DEMAND

First, consider the relationship between local and global ductility demands for a single-mass two-spring system, shown in Fig. 1. This relationship will be useful in later derivations. The ''weak link'' spring of initial stiffness K_w and the ''protected'' spring of stiffness K_p are connected in series. From a capacity design perspective, it is assumed that the ''weak link'' spring exhibits elastic-perfectly-plastic (EPP) behavior and has a finite yield strength $V_{w,y}$ smaller than that of the ''protected'' spring.

It is apparent, that the yield strength V_y of the system is equal to $V_{w,y}$. The yield displacement Δ_y of the mass consists of the local yield displacement ($\Delta_{w,y} = V_y/K_w$) of the ''weak link'' spring and the displacement contribution ($\Delta_p = V_y/K_p$) of the ''protected'' spring

$$\Delta_y = \Delta_{w,y} + \Delta_p = \frac{V_y}{K_w} + \frac{V_y}{K_p} \tag{1}$$

It follows from the above definitions that $V_y = K_w\Delta_{w,y} = K_p\Delta_p$, and

$$\frac{K_w}{K_p} = \frac{\Delta_p}{\Delta_{w,y}} \tag{2}$$

If the system undergoes inelastic deformation under applied dynamic force, or when subjected to support excitation, the peak displacement $\Delta_{\max}$ of the mass consists of the peak displacement contributions $\Delta_{w,\max}$ and $\Delta_{p,\max}$ provided by the ''weak link'' spring and the ''protected'' spring, respectively:

$$\Delta_{\max} = \Delta_{w,\max} + \Delta_{p,\max} \tag{3}$$

Since the strength of the system is limited by V_y, the displacement contribution $\Delta_{p,\max}$, of the ''protected'' spring is limited by V_y/K_p, therefore

$$\Delta_{p,\max} = \Delta_p = \frac{V_y}{K_p} \tag{4}$$

The local ductility demand μ_L for the ''weak link'' spring and the global ductility demand μ_G for the system are defined by

$$\mu_L = \frac{\Delta_{w,\max}}{\Delta_{w,y}} \tag{5}$$

$$\mu_G = \frac{\Delta_{\max}}{\Delta_y} \tag{6}$$

Substitution of (1) and (3) into (6) gives

$$\mu_G = \frac{\Delta_{w,\max} + \Delta_{p,\max}}{\Delta_{w,y} + \Delta_p} \tag{7}$$

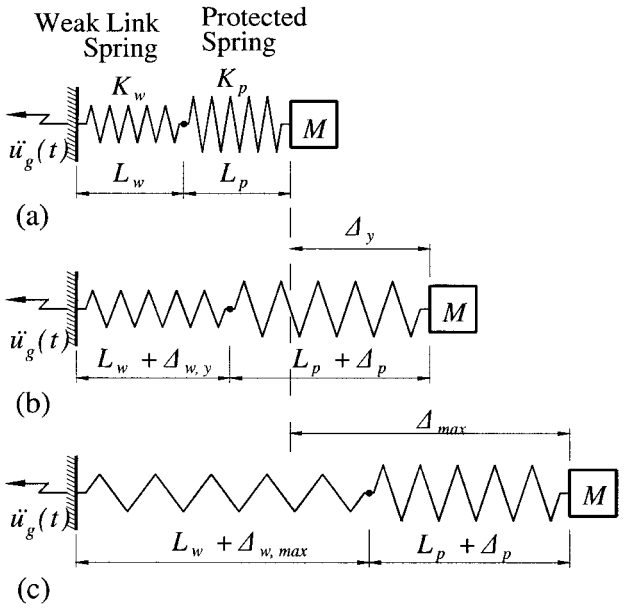

FIG. 1. Single-Mass Two-Spring System: (a) Initial Position; (b) at Yield; (c) at Maximum Displacement

Multiplication of both sides of (7) by $(\Delta_{w,y} + \Delta_p)/\Delta_{w,y}$ leads to

$$\mu_G + \mu_G \frac{\Delta_p}{\Delta_{w,y}} = \frac{\Delta_{w,\max}}{\Delta_{w,y}} + \frac{\Delta_{p,\max}}{\Delta_{w,y}} \tag{8}$$

Rearranging (8) and using (4) and (5), it can be shown that

$$\mu_L = \mu_G + (\mu_G - 1)\frac{\Delta_p}{\Delta_{w,y}} \tag{9a}$$

Using (2), the above expression can be rewritten as

$$\mu_L = \mu_G + (\mu_G - 1)\frac{K_w}{K_p} \tag{9b}$$

Eqs. (9) are valid for $\mu_G \geq 1$. Fig. 2 presents the plots of the normalized local ductility demands μ_L/μ_G for several common values of μ_G. It illustrates that the local ductility demand is larger than the global ductility demand for any nonzero positive finite value of K_p. If the ''protected'' spring is infinitely rigid ($K_p = \infty$), then $\mu_L = \mu_G$. Eqs. (9) can be expanded to accommodate any number of ''protected'' springs in the series. For a single mass system with $i + 1$ springs, where the single ''weak link'' spring has an initial stiffness K_w, and the i ''protected'' springs have stiffnesses $K_{p1}, K_{p2}, \ldots, K_{pi}$, (9*b*) can be written as

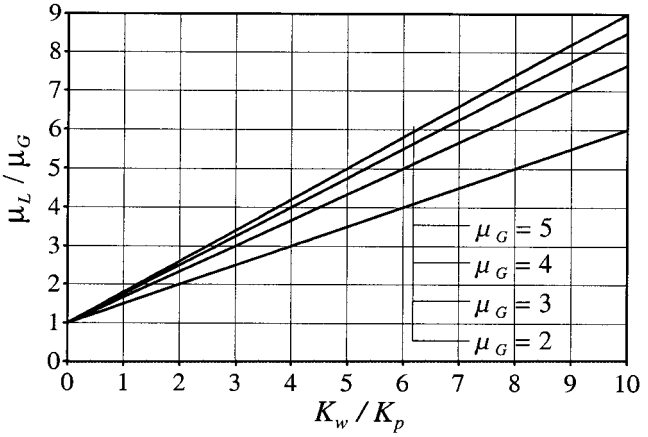

FIG. 2. Normalized Local Ductility Demands for Single-Mass Two-Spring System

$$\mu_L = \mu_G + (\mu_G - 1)\left(\frac{K_w}{K_{p1}} + \frac{K_w}{K_{p2}} + \cdots + \frac{K_w}{K_{pi}}\right) \tag{10}$$

which shows that, for a given global ductility demand, any additional flexibility in the ''protected'' part of the system adds to the local ductility demand imposed on the ''weak link'' spring. Note, the position of the ''weak link'' in the spring sequence within the series is of no importance.

Expressions similar to those of (9) can also be derived for ''weak link'' springs, exhibiting ductile behavior other than EPP. For example, if the ''weak link'' features a bilinear force-deformation relationship with a nonzero positive post-yield stiffness of $C_R K_w$ (where $0 < C_R < 1$ is a strain hardening coefficient), (9*b*) becomes

$$\mu_L = \mu_G + (\mu_G - 1)\frac{(1 - C_R)K_w}{K_p + C_R K_w} \tag{11}$$

In this case, to account for more than one ''protected'' spring in the series, K_p in (11) has to be substituted [in a similar manner as in (10)] by the equivalent stiffness, K_{pe}, of all ''protected'' springs that can be found from

$$\frac{1}{K_{pe}} = \frac{1}{K_{p1}} + \frac{1}{K_{p2}} + \cdots + \frac{1}{K_{pi}} \tag{12}$$

Numerical Example

Consider two highway bridges, shown in Fig. 3, with multiple 40-m long spans. The bridges have similar superstructures consisting of a 200-mm thick, 8-m wide, reinforced concrete deck resting on four simply supported WWF 1,200 × 333 steel girders spaced at 2 m. The mass of the superstructure is estimated to be 286×10^3 kg for one span including the mass of nonstructural elements (pavement, barriers, etc.). The substructures are reinforced concrete bents, each with four columns: (1) 900 mm in diameter for Bridge 1; and (2) 600 mm in diameter for Bridge 2. In this example, the bearings and the foundations are assumed infinitely rigid. The stiffnesses of the bents in the transverse direction of bridges are estimated to be 292 kN/mm and 32.4 kN/mm for Bridge 1 and Bridge 2, respectively.

Both bridges have ductile diaphragm panels that are installed between the two interior girders at the ends of each span. The use of diaphragms has been proposed as a seismic retrofit strategy in recent years, and detailed design procedures have been developed for that purpose (Sarraf and Bruneau 1998; Zahrai and Bruneau 1999). The objective of this strategy is to control seismic response in the transverse direction of the bridge by having a ductile fuse in the structure along the earthquake load path to protect, wherever possible, the superstructure and substructure from excessive loads. In this example, eccentrically braced frame (EBF) diaphragms are used, each with force-deformation characteristics approximated by EPP

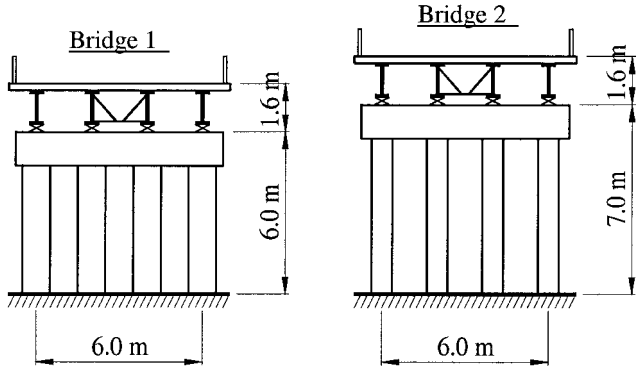

FIG. 3. Bridges 1 and 2 for Numerical Example

behavior with an initial stiffness of 92.05 kN/mm and yield strength of 254 kN. Flexibility of the superstructure between the end-diaphragms is negligible. The detailed description of these diaphragms is presented by Zahrai and Bruneau (1999).

For a quick estimate of the local ductility demands imposed on the diaphragms, the bridges can be modeled as single mass, two-spring systems similar to the one shown in Fig. 1 (the tributary mass of the superstructure is assumed lumped at the top of the two ductile diaphragm panels at each bent, and the mass of the bents is neglected). The two bridge systems have the following parameters in common: $M = 286 \times 10^3$ kg; $K_w = 184.1$ kN/mm; and $V_{w,y} = 508$ kN. For Bridge 1, $K_p = 292$ kN/mm, and for Bridge 2, $K_p = 32.4$ kN/mm.

For a given global ductility demand $\mu_G = 3$, it can be shown using (9*b*) that the local ductility demand for the diaphragms of Bridge 1 is 4.3, while the local ductility demand for the diaphragms of Bridge 2 is 14.4. For a given global ductility demand, the diaphragms will be subjected to higher ductility demands in bridges with more flexible bents.

Note that for Bridge 1, $K = 184.1 \times 292/(184.1 + 292) = 115.3$ kN/mm and $T = 2\pi \times (286/115{,}300)^{0.5} = 0.313$ s; whereas for Bridge 2, $K = 184.1 \times 32.4/(184.1 + 32.4) = 27.6$ kN/mm and $T = 2\pi \times (286/27{,}600)^{0.5} = 0.640$ s. For bridges with identical strength and subjected to given ground acceleration records, the longer period of Bridge 2 can usually (but not always) be associated with lower spectral pseudoacceleration and, thus, lower global ductility demands. For example, for the El Centro S00E acceleration record of the Imperial Valley 1940 event, scaled to 0.3 g, $\mu_G = 4.97$ for Bridge 1 and $\mu_G = 2.63$ for Bridge 2 (5% damping assumed). However, the corresponding local ductility demands for the current EBF diaphragms example determined using (9*b*) are $\mu_L = 7.5$ for Bridge 1 and $\mu_L = 11.9$ for Bridge 2. Therefore, even though the global ductility demand for Bridge 2 is almost twice as small than for Bridge 1, the local ductility demand for the diaphragms in Bridge 2 remains 1.6 times higher than in Bridge 1.

TRANSVERSE DYNAMIC RESPONSE OF A SYMMETRIC BEAM ON ELASTO-PLASTIC SUPPORTS

Consider a beam of length L [shown in Fig. 4(a)] with mass $m(x)$ and stiffness $EI(x)$ distributed symmetrically about the midspan. The beam is supported at the ends by two EPP springs of initial stiffness K_e and yield strength $V_{e,y}$ acting in the beam's transverse direction. Fig. 5(a) shows schematically a typical cycle of loading, unloading, and reloading for an end spring. The beam ends are free to rotate but completely restricted from translation in the beam's longitudinal direction. Both supports are subjected to the same earthquake induced acceleration history $\ddot{u}_g(t)$.

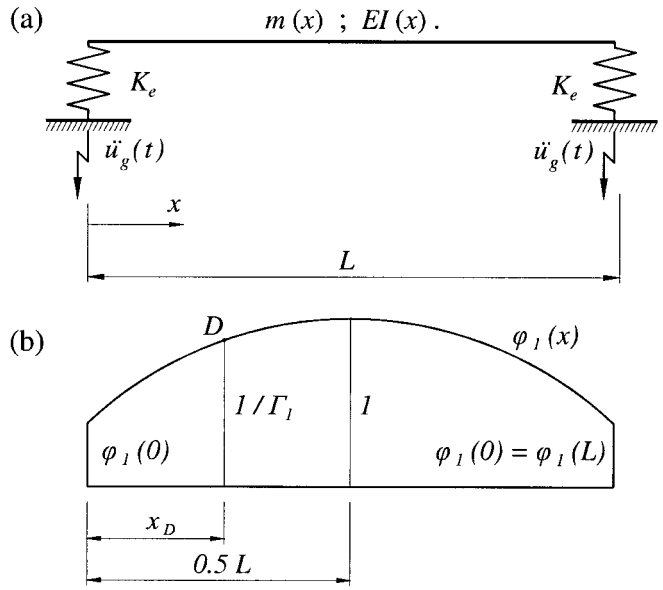

FIG. 4. (a) Symmetric Beam on Elasto-Plastic Supports; (b) First Mode Shape

The response of the considered beam is dominated by the first mode, and it can be analyzed with sufficient accuracy as a generalized SDOF system. Assuming classical damping for the first mode, the equation of motion (Chopra 1995) for the initial elastic response is

$$\ddot{z}_1(t) + 2\zeta_1\omega_1\dot{z}_1(t) + \omega_1^2 z_1(t) = -\Gamma_1\ddot{u}_g(t) \tag{13}$$

where ζ_1 is the damping ratio for the first mode, $z_1(t)$ is the generalized coordinate reflecting the displacement of the beam at midspan, and overdots denote time, t, derivatives. The first mode frequency and the modal participation factor are given by $\omega_1 = (K_1/M_1)^{0.5}$ and $\Gamma_1 = \Psi_1/M_1$, respectively, where

$$M_1 = \int_0^L m(x)[\varphi_1(x)]^2\,dx \tag{14a}$$

$$K_1 = \int_0^L \varphi_1(x)[EI(x)\varphi_1''(x)]''\,dx \tag{14b}$$

$$\Psi_1 = \int_0^L m(x)\varphi_1(x)\,dx \tag{14c}$$

Here, the primes denote derivatives with respect to spatial coordinate, x, along the beam, and $\varphi_1(x)$ is the first mode shape of the beam, where $\varphi_1(0.5\,L) = 1$. In the following derivation, it is convenient to use the normalized form of (13):

$$\ddot{D}(t) + 2\zeta_1\omega_1\dot{D}(t) + \omega_1^2 D(t) = -\ddot{u}_g(t) \tag{15}$$

where

$$D(t) = \frac{z_1(t)}{\Gamma_1} = \frac{z_e(t)}{\varphi_1(0)\Gamma_1} = \frac{2V_e(t)}{\omega_1^2 M_1^*} \tag{16}$$

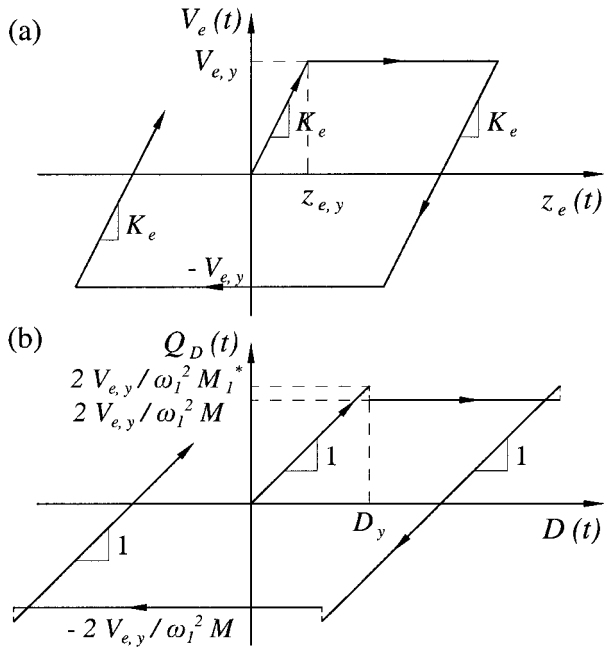

FIG. 5. Force-Deformation Relationships: (a) $V_e(t)$ versus $z_e(t)$; (b) $Q_D(t)$ versus $D(t)$

$M_1^* = \Gamma_1 \Psi_1$ is the effective modal mass, $V_e(t)$ is the restoring force in an end spring, and $z_e(t)$ is the displacement of beam ends. The yield displacement of the end springs is $z_{e,y} = V_{e,y}/K_e$, and the definitions for yield displacements D_y and z_{1y} follow from (16);

$$D_y = \frac{z_{e,y}}{\varphi_1(0)\Gamma_1} = \frac{2V_{e,y}}{\omega_1^2 M_1^*} \tag{17a}$$

$$z_{1y} = \frac{z_{e,y}}{\varphi_1(0)} = \frac{2V_{e,y}}{\omega_1^2 \Psi_1} \tag{17b}$$

The definition of $D(t)$ in (16) is valid for the initial elastic response only. In a more general sense, $D(t)$ can be associated with the displacement of point D at $x = x_D$, where $\varphi_1(x_D) = 1/\Gamma_1$, as shown in Fig. 4(b). Therefore, (15) can be extended to the inelastic range of response, and the equation of motion for the considered inelastic system can be written in terms of $D(t)$ as

$$\ddot{D}(t) + 2\zeta_1\omega_1\dot{D}(t) + \omega_1^2 Q_D(t) = -\ddot{u}_g(t) \tag{18}$$

where the normalized restoring force $Q_D(t)$ for the considered elastoplastic system is shown schematically in Fig. 5(b). During the initial elastic phase of the response, $Q_D(t)$ is equal to $D(t)$ of (16). During the yielding phase of the response, the beam is assumed to translate as a rigid body, effectively becoming an SDOF system with dynamic parameters $K_e = 0$, $M_1 = M$, $K_1 = 0$, $\Psi_1 = M$, $\Gamma_1 = 1$, and $M_1^* = M$ (where M is the total mass of the beam). The restoring force of the system is limited by $2V_{e,y}$, and when the end springs deform plastically

$$Q_D(t) = \frac{2V_{e,y}}{\omega_1^2 M} \tag{19}$$

The approximation of rigid body behavior follows from the dynamic equilibrium of the beam during the yielding phase of the response. This assumption was also examined in nonlinear analysis simulations by checking the deflected shape of the beam. In these simulations, the beam was modeled as a multiple degree of freedom (MDOF) system with supports subjected to a single pulse or an earthquake-induced acceleration history. The results indicate that the displacement of the midspan with respect to beam ends remains close to $[1 - \varphi_1(0)]z_{1y}$ during the plastic deformation of the end springs. Further, normalizing (18) by D_y, the ductility equation for the considered inelastic generalized SDOF system is obtained in terms of the normalized displacement $\mu_D(t)$

$$\ddot{\mu}_D(t) + 2\zeta_1\omega_1\dot{\mu}_D(t) + \omega_1^2 Q_\mu(t) = -\frac{\omega_1^2}{\eta_D}\frac{\ddot{u}_g(t)}{\ddot{u}_{g,\max}} \tag{20}$$

where

$$\mu_D(t) = \frac{D(t)}{D_y} \tag{21}$$

$$Q_\mu(t) = \frac{Q_D(t)}{D_y} \tag{22}$$

$$\eta_D = \frac{\omega_1^2 D_y}{\ddot{u}_{g,\max}} = \frac{2V_{e,y}}{M_1^* \ddot{u}_{g,\max}} \tag{23}$$

and $\ddot{u}_{g,\max}$ is the peak ground acceleration of the ground acceleration history $\ddot{u}_g(t)$.

The relationship between $Q_\mu(t)$ and $\mu_D(t)$ is shown schematically in Fig. 6(a). Eq. (20) can be solved numerically for $\mu_D(t)$ history, and an appropriate computer code could be developed to account for the discontinuity in $Q_\mu(t)$ at each time instant when the system goes from nonyielding to yielding states or from yielding to nonyielding states. However, by enforcing a continuous $Q_\mu(t)$, it is possible to utilize the widely available programs for the nonlinear analysis of ordinary SDOF systems to obtain an approximate solution for the considered generalized system. Indeed (20) is similar to the ductility equation governing the nonlinear response of a SDOF (not generalized) system having frequency ω_1, damping ratio ζ_1 and η-value parameter η_D. Such a SDOF system, however, has the $Q_\mu(t)$ versus $\mu_D(t)$ relationship shown in Fig. 6(b) instead of the one shown in Fig. 6(a) for the generalized system considered. The error in this approximation would depend on the magnitude of M_1^*/M in a likely non-linear manner. The approximated SDOF model is ''stronger'' than the original generalized system, because it has a higher value of $Q_\mu(t)$ during yielding. Therefore it would tend to underestimate μ_D, the peak value of the normalized displacement $\mu_D(t)$.

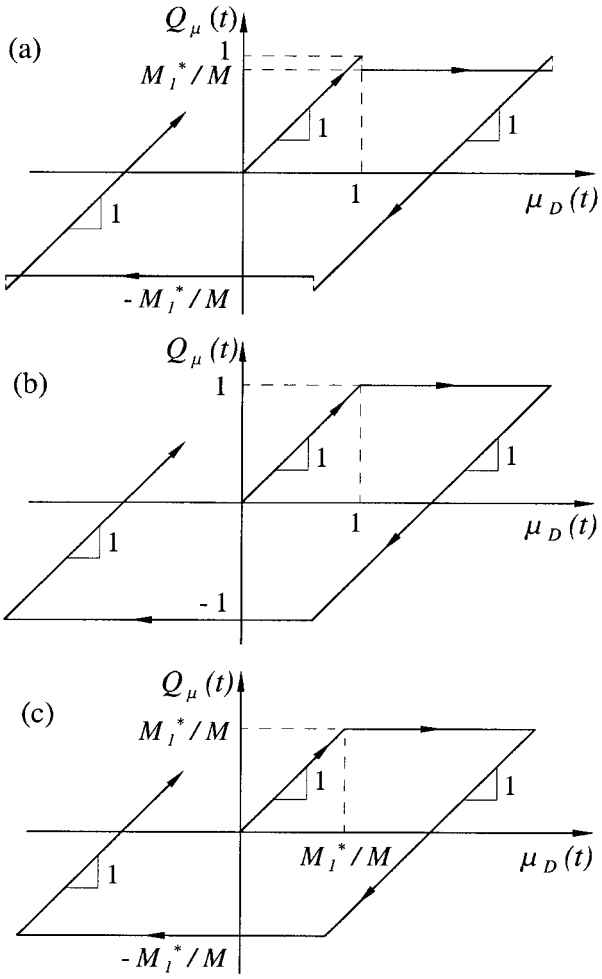

FIG. 6. $Q_\mu(t)$ versus $\mu_D(t)$ Relationships: (a) Generalized SDOF Model; (b) Approximated Model with η_D; (c) Approximated Model with η_a

A more conservative approximation can be achieved by adopting a SDOF model with the $Q_\mu(t) - \mu_D(t)$ relationship shown in Fig. 6(c), which implies an adjusted η-value parameter

$$\eta_a = \eta_D \frac{M_1^*}{M} = \frac{2V_{e,y}}{M\ddot{u}_{g,\max}} \tag{24}$$

This adjusted SDOF model has the same $Q_\mu(t)$ value during yielding as the original generalized system. However, it is ''weaker'' than the original system, because it has adopted lower yield displacement; therefore, it will tend to overestimate μ_D. It should also be mentioned that η_a of (24) is equal to the η-value of an inelastic SDOF model that assumes an infinitely rigid beam ($EI(x) = \infty$), i.e., $\eta_a = \eta_{(\text{RIGIDBEAM})}$. How-

ever, the SDOF models implied by Figs 6(b and c), are much better approximations of the investigated inelastic system than the rigid beam model, because these two models utilize the accurate value of the fundamental frequency ω_1 suggested by the generalized system.

The peak normalized displacement μ_D can be found from inelastic response time history analysis (or from earthquake or design ductility spectra) using one of the two approximate SDOF models. In most cases, the model with η_a produces more conservative results than the model with η_D. Then, by analogy with (9*a*), the local ductility demand μ_e in the end springs (i.e., the peak value of the normalized displacement $z_e(t)/z_{e,y}$) can be estimated from

$$\mu_e = \mu_D + (\mu_D - 1)\frac{1 - \varphi_1(0)\Gamma_1}{\varphi_1(0)\Gamma_1} = 1 + \frac{(\mu_D - 1)}{\varphi_1(0)\Gamma_1} \quad (25)$$

In a similar manner, the global ductility demand μ_G associated with the peak value of the normalized displacement $z_1(t)/z_{1y}$ at the midspan of the beam, can be evaluated from

$$\mu_G = 1 + \frac{(\mu_D - 1)}{\Gamma_1} \quad (26)$$

Eqs. (25) and (26) are valid for $\mu_D \geq 1$. For a beam of finite rigidity ($EI(x) \neq \infty$), $\Gamma_1 > 1$ and $\varphi_1(0)\Gamma_1 < 1$; therefore, these equations imply $\mu_e \geq \mu_D \geq \mu_G$.

BRIDGE DESIGN IMPLICATIONS

Current bridge design regulations (AASHTO 1998) use response modification factors R to reduce seismic design forces for substructure components. For symmetric simply supported spans, such R-factors can be interpreted as design ductility demands associated with μ_D. However, as it follows from (25), the local ductility demands for bridge supports are higher than μ_D. Therefore, current R-factors can be unsafe for bridges with flexible superstructures.

To illustrate this point, the case for a uniform superstructure (with $m(x) = m$, and $EI(x) = EI$) is considered here in more detail. The single-mode spectral method of seismic analysis (AASHTO 1998) based on a uniform loading shape, implies

$$\varphi_1(x) = \frac{3.2(xL^3 - 2x^3L + x^4 + 12BL^4)}{L^4(1 + 38.4B)} \quad (27)$$

where

$$B = \frac{EI}{K_e L^3} \quad (28)$$

Substitution of (27) in (14) leads to

$$\Gamma_1 = \frac{(1 + 38.4B)(60B + 1)}{38.4(60B^2 + 2B + 31/1512)} \quad (29)$$

$$M_1^* = \frac{M(60B + 1)^2}{60(60B^2 + 2B + 31/1512)} \quad (30)$$

$$T_1 = \frac{2\pi}{\omega_1} = 2\pi\sqrt{\frac{M(30B^2 + B + 31/3024)}{K_e B(60B + 1)}} \quad (31)$$

$$\varphi_1(0) = \frac{\omega_1^2 \Psi_1}{2K_e} = \frac{0.32B(60B + 1)^2}{(1 + 38.4B)(30B^2 + B + 31/3024)} \quad (32)$$

It should be noted, that (32) for the calculation of $\varphi_1(0)$ gives an improved accuracy over the direct use of (27) for the same purpose. Eqs. (29)–(32) provide convenient closed-form approximate expressions for the first mode dynamic parameters of interest and produce accurate results (Alfawakhiri and Bruneau 2000). The variation of these dynamic parameters, depending on the magnitude of the dimensionless stiffness index B, is illustrated in Fig. 7; Γ_1 and $\varphi_1(0)$ are non-dimensional parameters; other parameters are shown in normalized form. It can be observed from Fig. 7 that Γ_1 varies between 1.0 and $4/\pi$. The range of M_1^*/M is from $8/\pi^2$ at $B = 0$ to unity at $B = \infty$. The fundamental period T_1 is shown normalized by the period of a spring supported infinitely rigid beam ($EI = \infty$)

$$T(RIGID\ BEAM) = 2\pi\sqrt{\frac{M}{2K_e}} \quad (33)$$

The variation of the ratio, $[1 - \varphi_1(0)\Gamma_1]/\varphi_1(0)\Gamma_1$ depending on the magnitude of B, is illustrated in Fig. 8. This figure also presents the plots [based on (25)] of the normalized ductility demands μ_e/μ_D for several common values of μ_D. As can be observed from these plots, the ductility demand μ_e for the end springs is significantly larger than μ_D, especially in the lower range of B (i.e., for more flexible superstructures).

Based on the previous discussion, the following simple analytical procedure is recommended for a quick and fairly accurate (and conservative) evaluation of support ductility demands for symmetric simply supported bridges with flexible superstructures. For a bridge system with given $m(x)$, $EI(x)$, K_e, L, ζ_1 and $V_{e,y}$:

1. Determine $\varphi_1(x)$ for a uniform loading shape, then calculate K_1, M_1 and Ψ_1 using (14); this step is not necessary for the case of a uniform superstructure.
2. Determine Γ_1, M_1^*, T_1 and $\varphi_1(0)$, using results of step 1 [(28)–(32) for the case of a uniform superstructure].
3. Determine η_D using (23); alternatively, determine η_a, us-

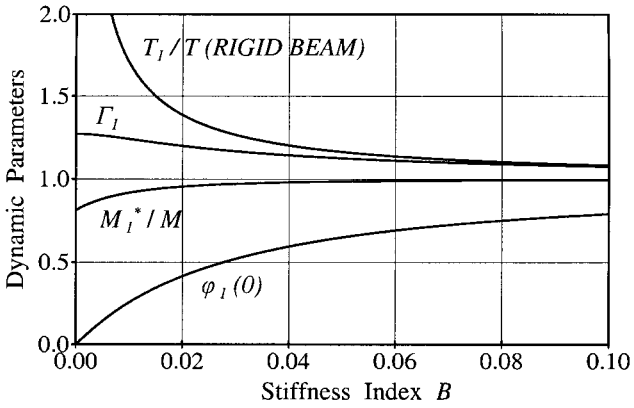

FIG. 7. First Mode Parameters for Uniform Beam on Elastic Supports

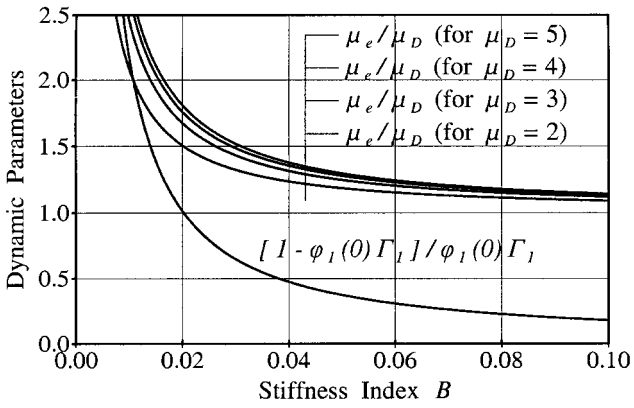

FIG. 8. Normalized Ductility Demands for End Supports (Uniform Beam)

ing (24) for a more conservative estimate of ductility demand.
4. For given ζ_1, and for T_1 and η_D (or η_a) determined in steps 2 and 3, find μ_D either by conducting a SDOF system time history analysis for a given ground motion, or directly from earthquake or design ductility spectra.
5. Finally, using (25) (or Fig. 8), determine the ductility demand μ_e for the bridge supports.

The end springs of the generalized model [Fig. 4(a)] can also represent several springs connected in series. As such, the force-deformation relationship of the inelastic end springs of the considered generalized model may be chosen to reflect the cumulative deformations of various bridge components that contribute to translation of the superstructure in the horizontal transverse direction (e.g., translation and rotation of foundations, bending and shear deformations of piers, bearings, and end diaphragms). However, bridge supports are usually designed to have only one weak link component to undergo inelastic deformations during strong earthquakes, while the other components are designed to respond elastically. In such cases, the local ductility demand μ_L for the weak link within the bridge support system itself (i.e., the weak link within an end spring of Fig. 4(a), if that spring stands for a series of springs) can be determined using (10) with μ_G substituted by μ_e, determined from step 5 above.

Numerical Example

Consider a multispan two-lane highway bridge, shown in Fig. 9(a), with each span 70-m long. The superstructure of the bridge consists of a 200-mm thick, 8-m wide, reinforced concrete deck resting on four simply supported WWF 1,800 $\times$ 632 steel girders, spaced at 2 m. For this example, the diaphragms within the superstructure, the bearings, and the foundations are assumed infinitely rigid. The ductile response of the supporting reinforced concrete bents in the transverse direction is approximated by an EPP force-deformation relationship (for each bent) with an initial stiffness of 168,820 N/mm and a yield strength of 1,920 kN. The mass of the superstructure, estimated to be 588×10^3 kg for one span, including the mass of nonstructural elements (pavement, barriers, etc.), is assumed uniformly distributed along the span. The combined stiffness of the bridge deck and the steel beams in the transverse direction is estimated to be 5.02×10^{17} N mm. Only a single span of the bridge is analyzed using the following parameters: $M = 588 \times 10^3$ kg; $K_e = 84{,}410$ N/mm; $L = 70 \times 10^3$ mm; $EI = 5.02 \times 10^{17}$ N mm^2; $\zeta_1 = 5\%$; $V_{e,y} = 960 \times 10^3$ N.

The ductility demand for the bents is evaluated for five different earthquake acceleration records using the following four models:

1. MDOF model shown in Fig. 9(b)
2. Rigid beam on inelastic springs SDOF model, i.e., assuming $EI = \infty$ for the superstructure
3. Approximated generalized SDOF model with η_D (23)
4. Approximated generalized SDOF model with η_a (24)

The earthquake acceleration records (Table 1) used for time-history analysis were all scaled to the peak ground acceleration of 0.5 g. These acceleration records were selected because, for the considered system (at periods of interest), they produce average ductility demands consistent with studies considering larger databases (Miranda and Bertero 1994).

The inelastic response time history analysis of the MDOF model was conducted utilizing DRAIN-2DX program (Prakash et al. 1993). For the other three models, the NONSPEC program (Mahin and Lin 1983), which directly gives SDOF peak ductility values, was used. Inelastic response time history analysis results are summarized in Table 2. The results of the MDOF model are considered ''exact,'' and the results of other models are compared to them.

The two approximated generalized SDOF models produce relatively accurate and conservative results for μ_e in almost all considered cases. The average local ductility demands predicted by these models are consistently close (within 15%) to the average ductility demand predicted by the MDOF model. Such level of accuracy is acceptable for many practical applications, in the perspective of estimating inelastic seismic response of bridges. It can also be observed from Table 2 that the approximated model with η_a is more conservative than the model with η_D.

In contrast to the approximated generalized SDOF models, the frequently used rigid beam SDOF model significantly underestimates the ductility demands for the bents in all considered cases. The average ductility demand predicted by the

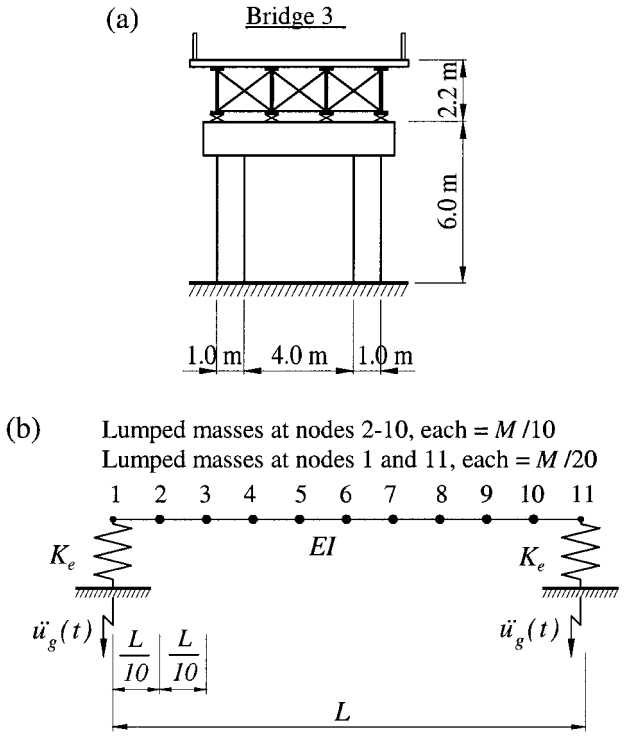

FIG. 9. (a) Bridge 3 for Numerical Example; (b) MDOF Model

TABLE 1. Earthquake Acceleration Records for Analysis

Event	Date (year-month-day)	Site	Peak ground acceleration (g)	Peak ground velocity (m/s)	Duration (s)
Whittier	87-10-01	Long Beach, Station 14242 (channel 1)	0.24	0.19	20
Loma Prieta	89-10-17	Capitola FS, Station 47125 (channel 1)	0.40	0.31	20
Cape Mendocino	92-04-25	Petrolia, Station 89156 (channel 3)	0.59	0.48	20
Landers	92-06-28	Joshua Tree, Station 22170 (channel 1)	0.28	0.43	30
Northridge	94-01-17	Castaic Route, Station 24278 (channel 3)	0.51	0.53	15

TABLE 2. Bridge 3—Inelastic Response Time History Analysis Results

Ground motion acceleration record (scaled to 0.5 g)	MDOF Model (DRAIN-2DX) $z_{e,y}$ = 11.37 mm		Rigid Beam SDOF Model (NONSPEC) T = 0.371 s; η = 0.666		Approximated Generalized SDOF Models (NONSPEC) T_1 = 0.534 s; Γ_1 = 1.209; $\varphi_1(0)$ = 0.378; M_1^*/M = 0.948					
					η_D = 0.701			η_a = 0.666		
	Peak $z_e(t)$ (mm)	μ_e	μ_e	Error (%)	μ_D	μ_e	Error (%)	μ_D	μ_e	Error (%)
Whittier	43.76	3.85	2.61	−32.2	2.62	4.54	+17.9	2.67	4.65	+20.7
Loma Prieta	88.40	7.77	4.83	−37.8	4.23	8.07	+3.9	4.76	9.23	+18.8
Cape Mendocino	64.16	5.64	4.04	−28.4	3.27	5.97	+5.9	3.53	6.54	+16.0
Landers	102.33	9.00	7.51	−16.6	4.61	8.90	−1.1	6.13	12.22	+35.8
Northridge	140.38	12.35	5.73	−53.6	5.36	10.54	−14.7	5.80	11.50	−6.9
Average	87.81	7.72	4.94	−36.0	4.02	7.60	−1.6	4.58	8.83	+14.4

MDOF model is 56% larger than that predicted by the rigid beam SDOF model.

Assuming that the response modification factor R = 5, specified for multiple column bents (AASHTO 1998), implies a design ductility capacity of 5, the μ_D values in Table 2 show compatible ductility demands. However, the average local ductility demand μ_e predicted by the MDOF model, is about 54% larger than the design ductility capacity of the bents. Indeed, R-factors in current bridge design regulations are tied to ductility demands anticipated for simple SDOF systems and fail to account for the higher local ductility demands that could be imposed on bridge supporting elements during an earthquake, as demonstrated here. Finally, note that railroad bridges that generally have narrow flexible spans could also provide fine examples to illustrate the above methodology.

CONCLUSIONS

In an inelastic structure for a given global ductility demand, introduction of a flexible elastic (i.e., capacity-protected) element in series along the earthquake load path increases the local ductility demand for the yielding element. A flexible substructure or superstructure in a bridge frame is no exception. In that perspective, the inelastic dynamic response of symmetric simply supported bridges to transverse ground motion was investigated. First, closed-form expressions that capture interaction of local and global ductility demands were derived and used to show how substructure flexibility increases the ductility demand in ductile end diaphragm systems. Secondly, it was shown how span-to-substructure relative flexibility can significantly increase ductility demand in bridge supports/substructure. A simplified method was developed to account for these effects in the inelastic analysis of bridges. Numerical case studies were presented to illustrate the new analytical tool.

The equations and figures in this paper can be used to determine in which instances the simplified approaches could be used and where it is recommended that the substructure and superstructure flexibilities be considered. This is important because, in the presence of flexible superstructures, the seismically-induced local ductility demands on bridge substructures could greatly exceed the ductility demands anticipated using the response modification factors (R-factors) in current bridge design specifications. Finally, although this study was limited to symmetric simply supported bridges, the effects associated with superstructure flexibility (period elongation and higher support ductility demands) would also be present in nonsymmetric and continuous bridges.

ACKNOWLEDGMENTS

The Natural Sciences and Engineering Research Council of Canada is acknowledged for its financial support through a Collaborative Grant on Innovative Seismic Retrofit of Existing Bridges. Farid Alfawakhiri gratefully acknowledges the Ontario Graduate Scholarship from the Ontario Ministry of Education and Training.

REFERENCES

Alfawakhiri, F., and Bruneau, M. (2000). ''Flexibility of superstructures and supports in the seismic analysis of simple bridges.'' *Earthquake Engrg. and Struct. Dyn.*, 29(5), 711–729.

Ballard, T. A., Krimotat, A., Mutobe, R., and Treyger, S. (1996). ''Nonlinear seismic analysis of Carquinez Strait bridge.'' *Rep. No. UCB/CEE-Steel-96/09*, University of California, Berkeley, Calif., 359–368.

Bridge design specifications. (1993). California Department of Transportation, Sacramento, Calif.

Chopra, A. K. (1995). *Dynamics of structures, theory and applications to earthquake engineering*, Prentice-Hall, Englewood Cliffs, N.J.

Dameron, R. A., Sobash, V. P., and Parker, D. R. (1995). ''Seismic analysis of the existing San Diego–Coronado Bay Bridge.'' *Rep. Prepared for California Department of Transportation*, Anatech Consulting Engineers, San Diego.

Donikian, R., Luo, S., Alhuraibi, M., Coke, C., Williams, M., and Swatta, M. (1996). ''The global analysis strategy for the seismic retrofit design of the San Rafael and San Mateo Bridges.'' *Rep. No. UCB/CEE-Steel-96/09*, University of California, Berkeley, Calif., 405–415.

Guide specifications for seismic isolation design. (1991). American Association of State Highway and Transportation Officials, Washington, D.C.

''Improved seismic design criteria for California bridges: Provisional recommendations.'' (1996). *Rep. No. ATC-32*, Applied Technology Council, Redwood City, Calif.

Ingham, T. J., Rodriguez, S., Nader, M. N., Taucer, F., and Seim, C. (1996). ''Seismic retrofit of the Golden Gate Bridge.'' *Rep. No. UCB/CEE-Steel-96/09*, University of California, Berkeley, Calif., 145–164.

Mahin, S., and Lin, J. (1983). ''Construction of inelastic response spectra for single-degree-of-freedom systems: Computer program and applications.'' *Rep. No. UCB/EERC-83/17*, Earthquake Engrg. Res. Ctr., University of California, Berkeley, Calif.

Miranda, E., and Bertero, V. V. (1994). ''Evaluation of strength reduction factors for earthquake-resistant design.'' *Earthquake Spectra*, 10(2), 357–379.

Prakash, V., Powell, G. H., and Campbell, S. (1993). ''DRAIN-2DX: Base program description and user guide, Version 1.10.'' *Rep. No. UCB/SEMM-93/17*, University of California, Berkeley, Calif.

Priestley, M. J. N., Seible, F., and Calvi, G. M. (1996). *Seismic design and retrofit of bridges*, Wiley, New York.

Sarraf, M., and Bruneau, M. (1998). ''Ductile seismic retrofit of steel deck-truss bridges. II: Design applications.'' *J. Struct. Engrg.*, ASCE, 124(11), 1263–1271.

Standard specifications for highway bridges. (1996). American Association of State Highway and Transportation Officials, Washington, D.C.

Vincent, J., Abrahamson, T., O'Sullivan, M., Lim, K., Dameron, R., and Donikian, R. (1997). ''Analysis and design for the inelastic response of a major steel bridge.'' *Proc., 2nd Nat. Conf. on Bridges and Hwys.—Progress in Res. and Practice*, Sacramento, Calif., 541–555.

Zahrai, S. M., and Bruneau, M. (1999). ''Ductile end-diaphragms for seismic retrofit of slab-on-girder steel bridges.'' *J. Struct. Engrg.*, ASCE, 125(1), 71–80.